

Biomaterials

Original Article

Title: Enhanced Osseointegration by the Chemotactic Activity of Plasma Fibronectin for Cellular Fibronectin Positive Cells

Authors: Ryo Jimbo^{a,1}, Takashi Sawase^{a,1}, Yasuaki Shibata^{b,*}, Kazunari Hirata^c, Yoshitaka Hishikawa^d, Yasuhiro Tanaka^e, Kazuhisa Bessho^f, Tohru Ikeda^b and Mitsuru Atsuta^a

Authors' affiliations:

^aDivision of Applied Prosthodontics, Nagasaki University Graduate School of Biomedical Sciences, Nagasaki, Japan

^bDivision of Oral Pathology and Bone Metabolism, Nagasaki University Graduate School of Biomedical Sciences, Nagasaki, Japan

^cDivision of Oral and Maxillofacial Surgery, Nagasaki University Graduate School of Biomedical Sciences, Nagasaki, Japan

^dDivision of Histology and Cell Biology, Nagasaki University Graduate School of Biomedical Sciences, Nagasaki, Japan

^eDepartment of Advanced Materials Science, Faculty of Engineering, Kagawa University, Kagawa, Japan

^fDepartment of Oral and Maxillofacial Surgery, Graduate School of Medicine, Kyoto University, Kyoto, Japan

¹ Equally contributed to the experimental work.

*Reprint requests and corresponding author: Yasuaki Shibata, Division of Oral Pathology and Bone Metabolism, Nagasaki University Graduate School of Biomedical Sciences, Nagasaki, Japan Tel: +81 95 849 7646, Fax: +81 95 849 7647, email: siva@nagasaki-u.ac.jp

Funding Sources: This study was supported by a Grant-in-Aid for Exploratory Research (17659616).

Running Title: Plasma FN chemotaxis enhances osseointegration

Abstract: Plasma FN (pFN) is known to regulate cell growth, differentiation or survival of osteoblasts *in vitro*. It is also speculated to be important for the early phase of osseointegration, however its actual *in vivo* behavior is unknown. The objective of this study is to clarify the role of pFN during osseointegration. We developed a titanium ion-plated acrylic implant (Ti-acryl) for thin sectioning without removal of the implant. Either Ti-acryl or pFN-coated Ti-acryl (FN-Ti-acryl) was implanted in the mouse femur. Samples were taken on day 1 to day 7 and on day 14 after the operation, and were decalcified and paraffin embedded. The bone healing process and immunofluorescence localization of pFN and cellular fibronectin (cFN), a marker for fibroblastic cells were examined. Simultaneously, the effect of pFN on chemotaxis, proliferation and differentiation of bone marrow stromal cells (BMSCs) was analyzed *in vitro*. The *in vivo* results showed that faster direct bone formation was seen for the FN-Ti-acryl group compared to the Ti-acryl group. The *in vitro* results showed that, pFN significantly promoted BMSCs chemotaxis, however had no effect on proliferation or differentiation. The results indicate that pFN regulated chemotaxis of osteogenic cells and coating the implant with pFN enhanced earlier osseointegration.

Key words: Implant; Fibronectin; Osseointegration; Histomorphometry; Chemotaxis

1. Introduction

The faster acquisition of the direct bone to implant anchorage, or so-called osseointegration, is the key factor in the faster functional loading of the implant. Comprehensive efforts and strategies have enhanced osseointegration for increased implant stability [1,2]. For example, the modification of the physical characteristics of the implant by sandblasting or chemical treatment of the implant surface has remarkably improved osseointegration as compared to turned surfaces [3-5]. The reason for such improvement is speculated to be the enhanced adsorption of native blood proteins, such as plasma fibronectin (pFN), onto the implant surface, which enhanced the formation of focal adhesions by osteoblasts through integrin-mediated mechanisms [6,7].

Plasma FN is a prominent extracellular matrix protein [8], which accumulates in the matrix during the early phase of cell growth and attachment [9]. Cellular FN (cFN), another type of FN, is an insoluble form generated as a result of alternative splicing from a single gene [10]. It is expressed locally by certain fibroblastic cells and other cell types, and is deposited and assembled into the extracellular matrix [11]. It has been suggested that pFN activates the signaling pathways which direct cell-cycle progression, gene expression and matrix mineralization [12], and even regulating the survival of osteoblasts [13]. In fact, coating biomaterial surfaces with pFN in vitro has been shown to enhance the formation of focal adhesions by osteoblasts [14] and lead to better cell spreading and cytoskeleton organization compared to non-coated surfaces [15-17]. In addition, it has been reported that pFN adsorbed onto the implant surface when the

implant was inserted in the abdominal walls of rats [18]. This evidence suggests that the pFN adsorbed onto the implant surface regulates cellular adhesion and consequent osseointegration. Park *et al.* have reported that early blood cell/implant interactions which leads to plasma protein accumulation may play a key role in the osteoconduction stage of osseointegration [19]. Rupp *et al.* have discussed the possible FN adsorption onto endosseous implants via the patient's blood during surgery [20]. However, these reports were only speculations, and the actual behavior of FN at the molecular level in vivo around implants during the process of osseointegration remains uncertain. One of the reasons for this is the difficulty in making thin sections without the removal of the implant incorporated into the surrounding bone. Hence, most of the past studies were performed on undecalcified ground sections. Nevertheless, the ground sections clarified the osteoconductive bone regeneration process around the implants histologically and histomorphometrically [21,22], they did not allow for analysis at the molecular level.

We developed an implant coated with a thin film of titanium by means of the ion-plating method [23]. With this implant, the preparation of paraffin-embedded or frozen sections for immunohistochemistry or in situ hybridization is possible without removing the titanium implant. In the current study, by using this implant, the effects of pFN on the osseointegration process in the mice femur histologically and histomorphometrically was examined, followed by immunofluorescence observation with pFN antibody and cFN antibody. Simultaneously, the effect of pFN on bone marrow stromal cells (BMSCs) was examined in the in vitro studies.

2. Materials and Methods

2.1. Fabrication of the titanium-ion-plated acrylic implant

An acrylic rod (1.0 mm in diameter and 2.0 mm in length) was ultrasonically cleaned in ethanol and distilled water. The titanium-ion-plating methods were applied, based on our previous study [23]. Briefly, the specimens were placed for 10 minutes in an ion-plating apparatus (MODEL 1602EB; Ayers Rock Corp., Kanagawa, Japan) and were exposed to an argon gas plasma created under 100 W radio frequency power, 12-16 mPa argon gas pressure and 500 V bias voltage. The thickness of the plated titanium was fixed to approximately 20 nm and was confirmed by a cross sectional transmission electron microscope (JEM 3010; JEOL) at an accelerating voltage of 300 kV.

2.2. Surgical procedures

Ddy mice (8-week-old males, n=3) were anesthetized, a round bone defect 1.0 mm in diameter was created in the middle portion of the diaphysis of the left femur and the implants were inserted. The following two types of implants were used in the experiment:

1. Ti-acryl (control group): titanium-ion-plated acrylic implant;
2. FN-Ti-acryl (experimental group): titanium-ion-plated acrylic implant soaked in mouse plasma fibronectin (Biogenesis; concentration: 100 µg/ml) at 4 C° for 30 minutes.

The animals were sacrificed at 1, 2, 3, 4, 5, 7 and 14 days after the operation, the samples were perfusion-fixed with 4% paraformaldehyde (PFA) in phosphate-buffered saline (PBS), decalcified with 10% ethylenediaminetetraacetic acid and embedded in paraffin, and thin paraffin sections were prepared (thickness: 3 μ m). The sections were first observed histologically with hematoxylin and eosin (H&E) staining.

Animal care and experimental procedures were performed in accordance with the Guidelines for Animal Experimentation of Nagasaki University with the approval of the Institutional Animal Care and Use Committee.

2.3. Immunofluorescence staining and in situ hybridization

For the immunofluorescence staining, we prepared a rabbit anti-human pFN antibody according to the methods of Weiss *et al.* [24]. Additionally, as a marker for the fibroblastic cells, we used goat anti-human cFN antibody (C-20; Santa Cruz Biotechnology). The deparaffinized sections were first blocked with 1% bovine serum albumin (BSA) in PBS for 30 minutes at room temperature. The slides were incubated with the two primary antibodies diluted with PBS (1:200) for 2 hours at room temperature. After extensive washing with PBS, they were incubated with anti-rabbit fluorescein-linked whole antibody (GE Healthcare) and anti-goat Alexa Fluor 594 (Molecular Probe). The fluorescence signals were visualized using a confocal laser microscope (LSM5 PASCAL; Carl Zeiss).

In situ hybridization (ISH) was performed for both groups at day 4 in order to observe the osteogenic activity at the implant surface. For the probe preparation, the cDNAs of osteocalcin (Ocn) subcloned into pGEM-T Easy (Promega) were labeled with digoxigenin with either T7 or Sp6 RNA polymerase. The in situ hybridization was performed as described in our previous studies [25].

2.4. Histomorphometrical analysis

The area of the implant surface that was in contact with bone (bone-implant contact, BIC) was calculated at days 5 to 14. The percentages of bone in direct contact to the implant surface were determined.

The number of fibroblastic cells infiltrated around the implant was counted in a prescribed rectangular area for both groups (0.5 mm x 1.0 mm, adjacent to the implant surface).

Histomorphometric analysis was performed on all specimens using an image analyzing software (Image J ver.1.36b; National Institutes of Health).

2.5. Immunohistochemistry

The proliferation activity of the fibroblastic cells around the implant at day 2 was analyzed by immunostaining the proliferating cell nuclear antigen (PCNA). After preincubation with 1% H₂O₂ in methanol for 30 minutes, and blocking with 1% BSA,

the sections were incubated for 2 hours at room temperature with a 1:200 dilution of anti-PCNA antibody (PC10; DAKO). The sections were then incubated with the appropriate biotinylated secondary antibodies, followed by incubation with the avidin-biotin peroxidase complex (Vectastain Elite ABC kit; Vector). The peroxidase conjugates were subsequently localized using diaminobenzidine tetrahydrochloride as a substrate. The ratio of PCNA+ fibroblastic cells among all fibroblastic cells was calculated in a prescribed rectangular area (0.5 mm x 1.0 mm, adjacent to the implant surface).

2.6. Cell culture

The femurs and tibiae of the 8-week-old male ddy mice were cut at the epiphyses, and a BMSCs-rich fraction was obtained by flushing the diaphyseal channel with alpha-MEM (Gibco Laboratories) containing 10 % fetal calf serum, 100 µg/ml penicillin G and 100 IU/ml streptomycin through a 23-gauge needle. The cells were then filtrated with a 70-µm nylon filter (Cell Strainer; BD Bioscience), and cultured for 3 days in alpha-MEM containing 10 % FCS and antibiotics at 37 °C in 5 % CO₂. After 3 days of primary culturing, the non-adherent population was aspirated and the adherent cells were collected by scraping with a rubber wiper; the adherent cells were then concentrated by centrifugation at 1500 revolutions per minute (rpm) for 5 minutes at room temperature and resuspended.

2.7. Chemotaxis assay

To examine whether or not pFN induces the chemotaxis of fibroblastic cells in the bone marrow, the chemotactic responses were measured by means of a modified Boyden chamber assay, using a 24-well-type chamber equipped with polycarbonate filters having 8- μm pores (Chemotaxicell-24; Kurabo, Kurashiki, Japan). The lower side of the filter was coated with either pFN or type-I collagen (Coll; Cell Matrix, Nitta-Gelatin, Osaka, Japan) for 30 minutes at room temperature within a wide concentration range (from 100 ng/ml to 100 $\mu\text{g/ml}$). A non-coated filter was used as a control. The lower wells were filled with 600 μl of alpha-MEM, and the upper wells were filled with the obtained cells (40×10^4 cells/ml) in 200 μl of medium. After 24 hours of incubation, the filters were carefully removed and the non-migrating cells on the upper side were eliminated by gentle scraping with a rubber wiper and rinsing with cold PBS. The migrating cells on the lower side of the filter were fixed with PFA and stained with toluidine blue. The number of migrating cells was counted at 10 x magnification, and the procedure was repeated in triplicate.

2.8. In vitro proliferation assay

The cellular proliferation activity was estimated based on the uptake of bromo-deoxyuridine (BrdU). Polystyrene 96-well plates were coated with pFN (concentration: from 100 ng/ml to 100 $\mu\text{g/ml}$) at 4 °C for 30 minutes. The wells were then blocked with 1% BSA for 30 minutes at room temperature and rinsed with PBS before adding the cells. As a control, Coll-coated wells with the same concentration

range and non-treated wells were used. The cells were then added (40×10^4 cells/ml) and cultured for 24 hours. Cell viability was assessed by the Biotrak™ cell proliferation ELISA system (GE Healthcare), according to the manufacturer's instructions.

2.9. Analysis of osteogenic differentiation in vitro

In order to assess the osteoinductive role of pFN, BMSCs-rich fractions were cultured on pFN- or CollI-coated or non-coated dishes and transfected with adenoviral rh-BMP-2 [26]. After 4 days, the transfection-elevated alkaline phosphatase (ALP) production was compared among the three groups. The ALP activity was detected by enzyme histochemistry, as in our previous studies [27].

2.10. Statistical analysis

All statistical analyses in this study were performed with KaleidaGraph (Synergy Software). The mean and standard deviation values of the histomorphometric and in vitro parameters (n=3) were calculated. The average values were compared by one-way analysis of variance, followed by a *post hoc* Tukey test with the value of statistical significance set at the 0.05 level.

3. Results

3.1. Histological examination of the bone formation process for Ti-acryl and FN-Ti-acryl

In the Ti-acryl (control) group, the peri-implant bone healing proceeded as follows. At

day 1, the peri-implant tissue was edematous (Fig. 1A). At day 2, a dense fibrin layer was observed just outside of the implant surface; sparse infiltration of spindle-shaped fibroblastic cells was noticed outside of the fibrin layer (Figs. 1B). At day 3, the fibroblastic cells surrounded the implant surface (Figs. 1C). At day 4, new bone formation was seen in an area hemmed by the cortex and the implant; however, bone formation could not be observed at the implant surface; mononuclear cells or fibroblastic cells surrounded the surface of the implant (Figs. 1D and 1E); no expression of Ocn mRNA was observed at the implant surface (Fig. 1F). At day 5, the bone volume increased; however, layers of fibroblastic cells were still observed at the implant surface (Fig. 1G). At day 7, the bone volume increased further and at last, the bone was in direct contact with the implant surface (Fig. 1H). At day 14, the bone volume increased even further and the bone became compact (data not shown).

Whereas, in the FN-Ti-acryl (experimental) group, at day 1 the peri-implant tissue was less edematous than in the control group (Fig. 2A). At day 2, fibroblastic cells reached the implant surface and infiltrated the surrounding tissues (Figs. 2B). At day 3, a larger number of fibroblastic cells infiltrated the area around the implant compared to the Ti-acryl group (Fig. 2C). At day 4, deposition of bone matrix appeared directly on the implant surface, as well in an area hemmed by the cortex and the implant (Fig. 2D); osteoblastic cells rimming the matrix and osteocytic cells embedded in the matrix were observed under higher magnification (Figs. 2E and 2G); Ocn mRNA expression was detected in the cells at the bone-implant interface and in the bone matrix (Figs. 2F and

2H). At day 5, the bone matrix was in direct contact with the implant surface, without the intervention of any fibroblastic cells at the bone-implant interface, and the bone volume around the implant increased (Fig. 2I). At days 7 (Fig. 2J) to 14 (data not shown), the bone volume further increased and the bone became compact.

3.2. Bone-implant contact analysis

The BIC in the experimental group was significantly higher than those in the control group at day 5. In the control group, the BIC was 43.6 % and in the experimental group, the BIC was 81.6 %. There was no significant difference between the BIC values of these groups at days 7 and 14 (Figs 3A and 3B).

3.3. Infiltration of fibroblastic cells and PCNA proliferation assay

The total number of infiltrated fibroblastic cells in the experimental group was 1.86 times larger than that in the control group (Fig. 3C). The percentage of PCNA+ fibroblastic cells at day 2 was 20.5 % in the control group and 19.2 % in the experimental group. (Fig. 3D) There was no significant difference in the proliferation rates of the two groups.

3.4. Immunofluorescence staining

In the control group at day 1, pFN signals were detected, not around the entire implant surface, but chiefly in an area hemmed by the cortex and the implant (Fig. 4A). At day 2, the pFN signals disappeared at the implant surface, whereas they could still be detected

in the matrix away from the implant surface (Figs. 4B-4D). Strong cFN signals were detected in the fibroblastic cells; however, lower pFN signals were detected at the implant surface compared to the matrix away from the implant (Figs. 4C, 4E and 4F). The corresponding H&E stained sections show an infiltration of fibroblastic cells outside of the fibrin layer (Fig. 4G). At day 3, the pFN signals were drastically reduced (Fig. 4H) and the infiltration of cFN-negative fibroblastic cells could be seen at the implant surface (Figs. 4I-K). At day 4, both signals completely disappeared (data not shown).

In the experimental group at day 1, pFN immunofluorescence signals were detected extensively around the implant surface and in the surrounding matrix (Fig. 5A). At day 2, the pFN signals were still observable at the implant surface (Figs. 5B-5E); cellular-FN+ fibroblastic cells also reached the implant surface and infiltrated the surrounding matrix (Figs. 5C, 5E and 5F). The corresponding H&E sections show a direct infiltration of fibroblastic cells to the implant surface (Fig. 5G). At day 3, capillaries were generated in some places adjacent to the implant surface; the infiltration of cFN+ fibroblastic cells was also evident in this area (Figs. 5I-K), while pFN signals around the implant decreased (Fig. 5H). At day 4, both signals were still visible, but lower compared to those at day 3 (data not shown).

3.5. Effect of pFN on the chemotaxis, proliferation and osteo-differentiation of bone marrow stromal cells

The chemotaxis assay revealed that pFN significantly promoted the chemotaxis of BMSCs compared to the ColI-coated or non-coated chambers (Fig. 6A). Although the chemotactic activity of BMSCs increased in a dose dependent manner in both the pFN and the ColI-coated group, the chemotactic ratio in the pFN-coated group was significantly higher than that in the ColI-coated group at all concentrations tested. The BrdU-uptake of BMSCs cultured on the various groups of wells did not result in any significant differences in proliferation ratio (Fig. 6B). The histochemical analysis of the ALP enzyme revealed no drastic variance in ALP activity between any of the cells cultured on any well after the transfection of BMP-2 (Fig. 6C).

4. Discussion

This is the first report that addressed the *in vivo* localization and role of pFN during osseointegration. Our results demonstrated that coating the implant with pFN induced faster osseointegration compared to the non-coated implant, and suggested that this phenomenon was due to the recruitment of larger number of cFN⁺ BMSCs closer to the implant surface by the preferential chemotactic activity of pFN. Although the adsorption of blood proteins to the titanium implant has been suggested to play an important role for osseointegration [7,28], the actual *in vivo* localization of blood proteins and its role for osseointegration remained uncertain. In this study, we developed the paraffin-sectionable titanium ion-plated acrylic implant model for the detection of in

situ localization of molecules involved in osseointegration. The paraffin sections showed titanium film attached directly to the periimplant tissue, meaning the bone-implant or tissue-implant interface was well preserved.

During days 2-3, there was a drastic reduction of the pFN signal in the control group. In contrast, the pFN signal could still be detected at the implant surface in the experimental group. The pFN detected in the experimental group may be due to the release of pFN from the pFN coated implant. The histological results of this study show that, at day 2, the infiltration of a larger number of cFN+ BMSCs to the implant surface could be observed in the experimental group compared to the control group (Fig. 3C). At day 3, the infiltration of cFN+ BMSCs to the implant surface was evident only in the experimental group, and the cells which reached the implant surface in the control group were cFN-negative (Figs. 4I, K and 5I, K). In this study, cells with integrin receptors were speculated to migrate to the pFN accumulated implant surface, but the mechanisms of the preferential chemotaxis of the cFN+ BMSCs remained uncertain. However the results of this study indicated a close relationship between pFN and cFN+ BMSCs, as Hayman *et al.* have suggested [29] and furthermore, pFN was suggested to induce the preferential chemotaxis of cFN+ BMSCs. In addition, the histological results showed that the pFN-coated implant induced faster osseointegration. These results strongly suggest that the cFN+ BMSCs possess a higher tendency to differentiate into osteogenic cells.

The prominent vasculogenesis around the experimental implant may also have been the result of the chemotactic activity of pFN, because mice lacking FN die around embryonic day 8.5 due to severe defects in mesodermally derived tissues, including defects of vasculogenesis [30]. As vascularization is reported to be indispensable for osseointegration [31], further vasculogenesis induced by the administration of pFN may also accelerate osseointegration.

Osseointegration is defined as the direct anchorage of an implant due to the formation of bony tissue around the implant, without the growth of fibrous tissue at the bone-implant interface [31]. From the clinical point of view, during this process, two factors play an important role: primary stability (mechanical stability) and secondary stability (biological stability after bone remodeling) [32]. Primary stability is the mechanical stability of the implant as soon as the implant is placed into the bone. It gradually decreases in the bone remodeling process. Secondary stability is the contact of new bone with the implant after bone remodeling. Primary stability is fully replaced by secondary stability when the healing process is completed. However, at one point, the implant stability decreases during the stability conversion, a process also called the “dip”. Many implant failures occur during this period, and this period seems to be critical to the successful integration of the implant [33]. The results of this study suggest that the adsorption of pFN onto the implant surface advances the starting point of the achievement of secondary stability.

Coating the implant with pFN significantly enhanced osseointegration at days 4 and 5, however the results of the BIC analysis showed that there was no significant difference between the two groups at days 7 and 14, which mark the latter stages of bone regeneration. These results imply that pFN may be an important factor for the initial stages of osseointegration which have a profound impact on the bone-implant stability. Hence, strategies to induce the adsorption of pFN onto the implant would accelerate osseointegration and substantially reduce the stability dip if a sufficient amount of pFN can be adsorbed. There are two possible strategies for the progressive adsorption of pFN onto the implant surface. One is to mechanically coat the implant with pFN, as done in this study. The other is to physico-chemically modify the implant surface in order to render it optimal for further accumulation of the endogenic pFN. Deligianni *et al.* have stated that higher amounts of FN were found on rough titanium surfaces compared to smoother surfaces [34]. The surface roughness of the model we used in this study was $R_a=0.815$, a relatively smooth surface, and the reduction of the pFN signal could be seen by day 2 in the control group. It may well be useful to roughen the surface not only to ensure the longer duration of pFN around the implant but also to enable the mechanical coating of the implant surface with a larger amount of pFN.

The observed remarkable enhancement of new bone apposition on the pFN-coated implant surface during the initial stages of osseointegration is promising and could lead to a significant reduction of the healing period in clinical applications.

5. Conclusion

This current study using the newly developed titanium ion-plated acrylic implant experimental system showed that coating plasma fibronectin (pFN) onto the implant surface induced earlier osseointegration than that of the non-coated control. In vitro chemotaxis assay showed chemotaxis of cellular fibronectin (cFN)-positive bone marrow stromal cells by the effect of pFN. The in vivo and in vitro results suggested that adsorption of pFN onto the implant surface was effective for earlier osseointegration due to the release of pFN and for the subsequent chemotaxis of cFN-positive bone marrow stromal cells with an osteogenic potential.

Acknowledgments

This study was supported by a Grant-in-Aid for Exploratory Research (17659616).

Fig1

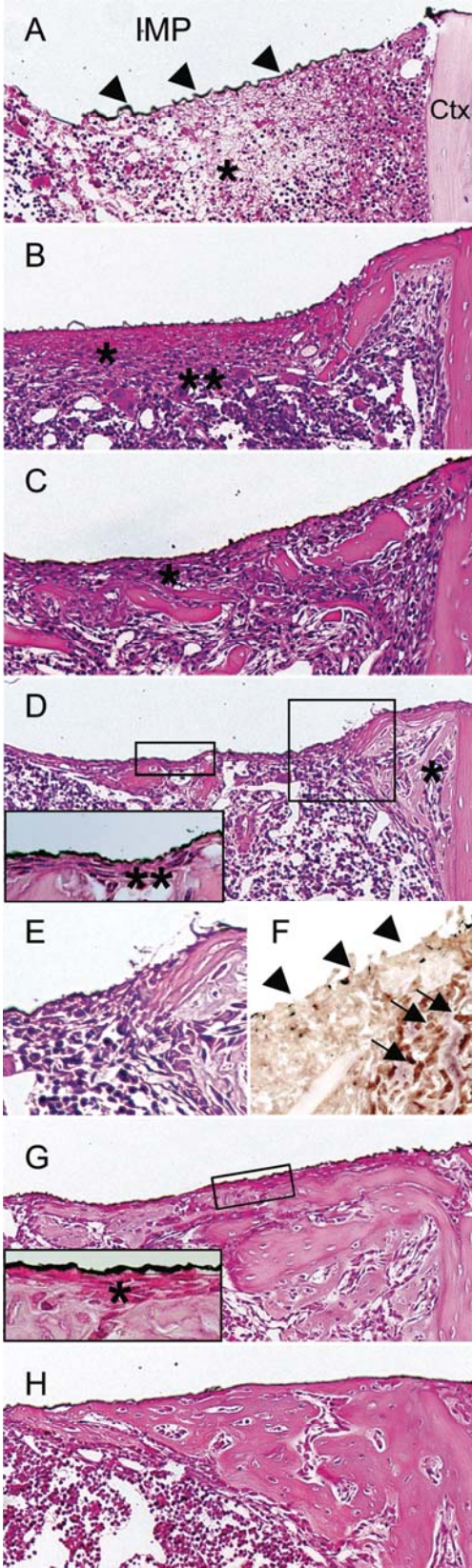


Fig2

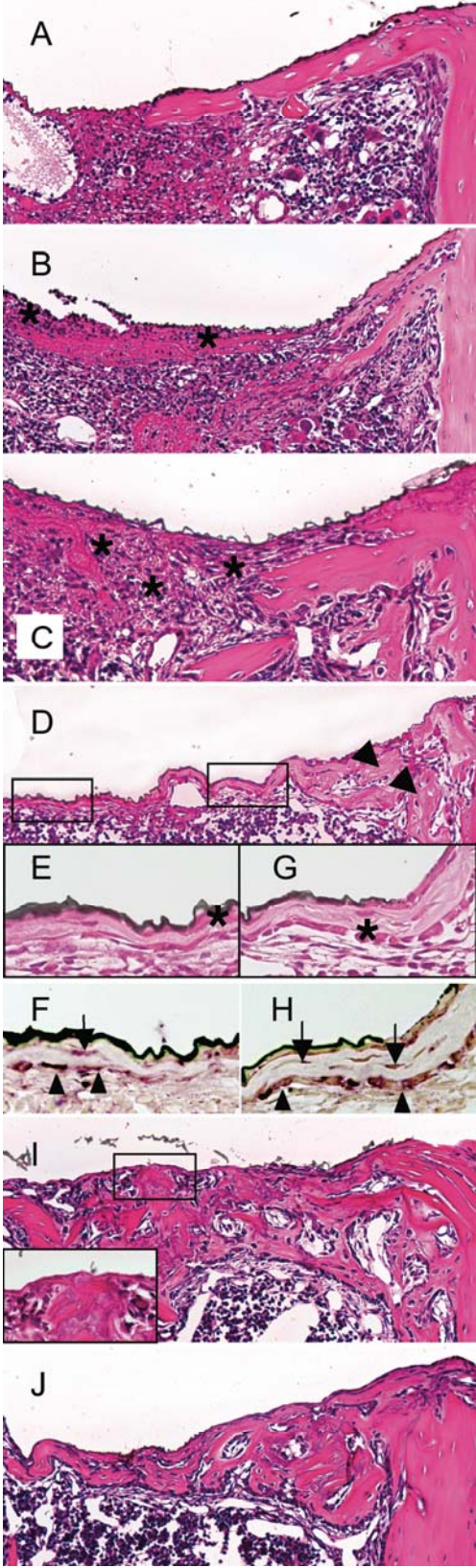


Fig3

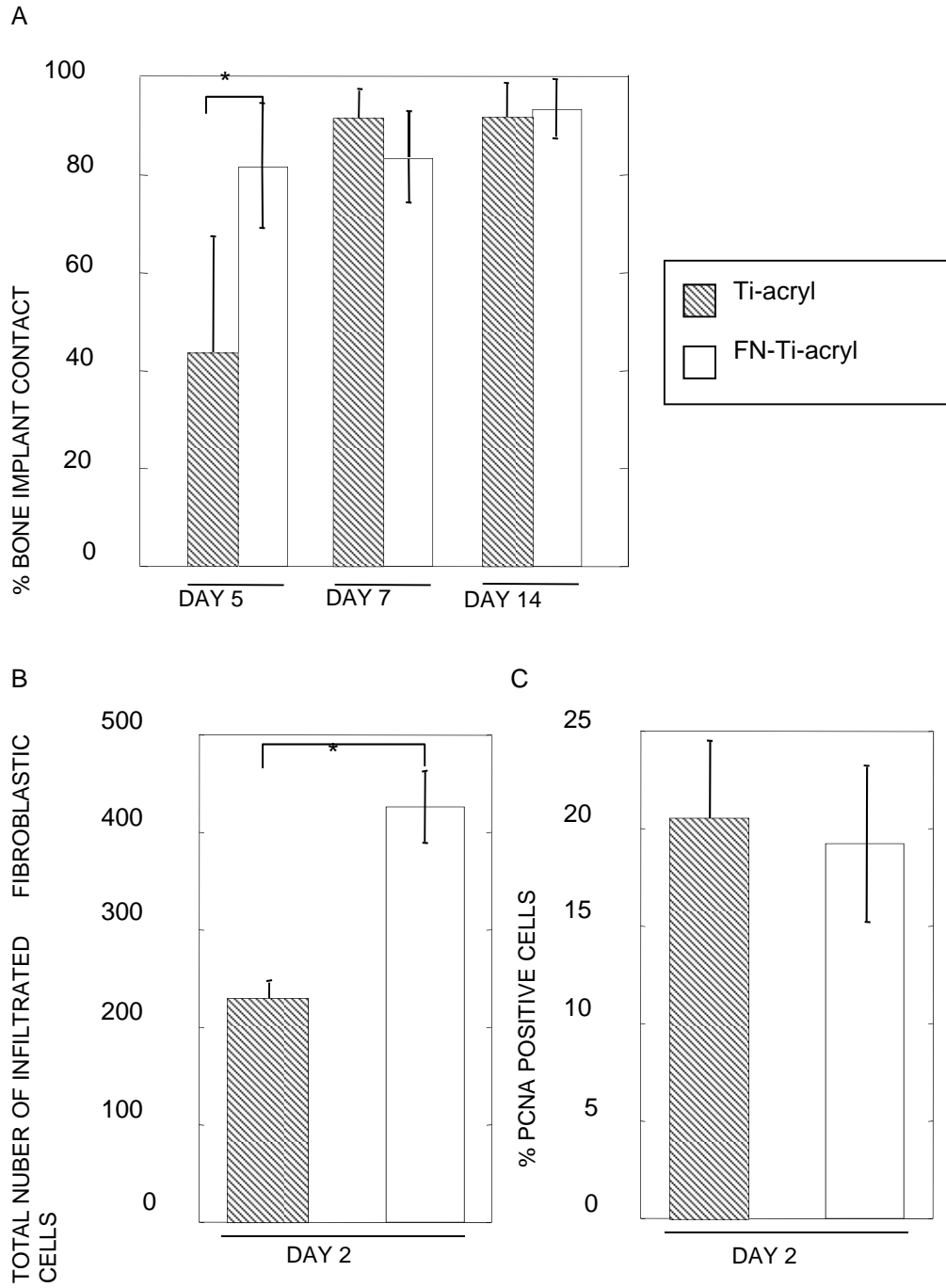


Fig4

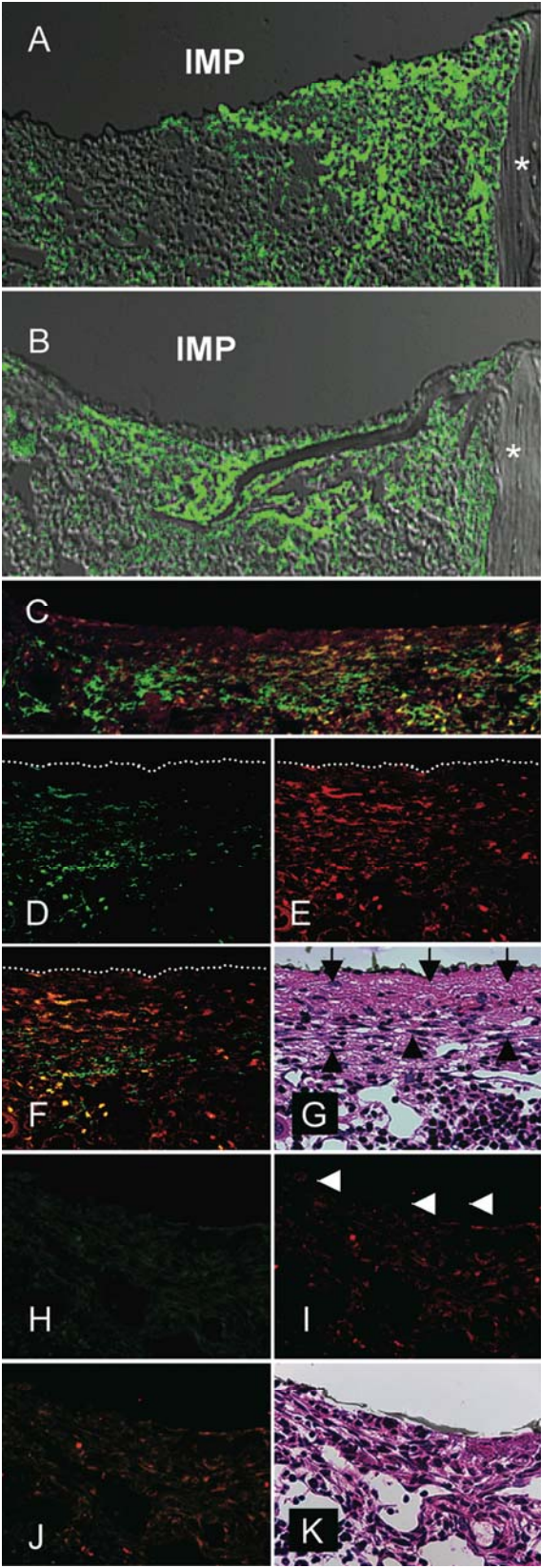


Fig5

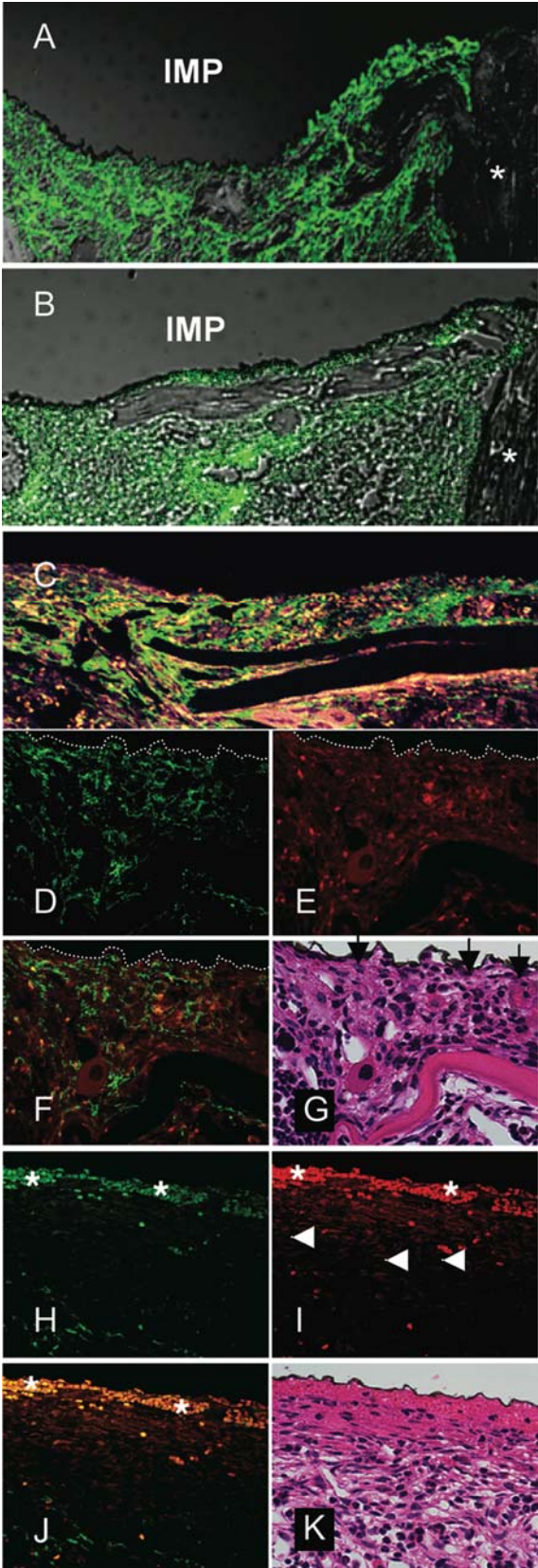


Fig6

